Supporting Information

Synthesis and Stabilization of Blue-Black TiO_2 Nanotube Arrays for Electrochemical Oxidant Generation and Wastewater Treatment

Yang Yang and Michael R. Hoffmann*

Linde + Robinson Laboratories

California Institute of Technology

1200 E. California Blvd.

MC 131-24

Pasadena, California 91125, United States

A manuscript submitted to ***Environ. Sci. Technol.***

*Corresponding author: Email: mrh@caltech.edu

This 14-page file contains eight figures, one table, and three texts.

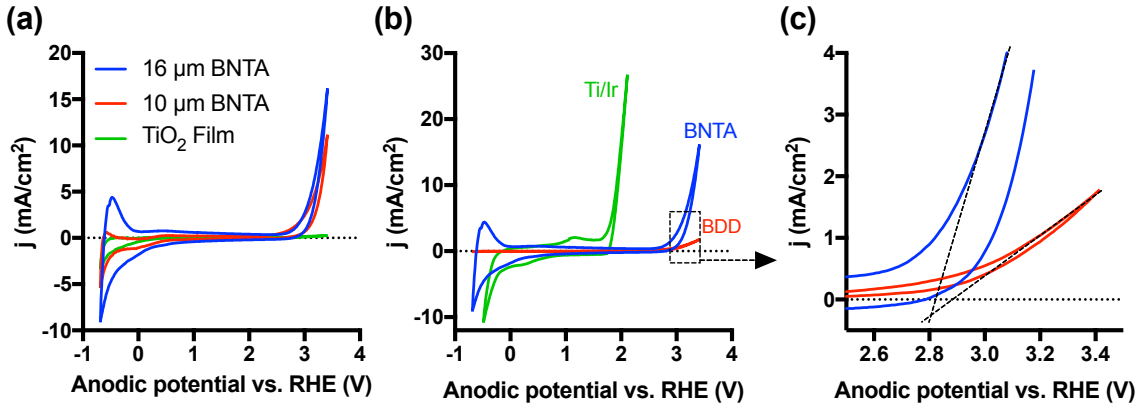

Figure S1. (a) Cyclic voltammetries of BNTA and TiO_2 film. TiO_2 film was deposited on a Ti base metal plate by spray-pyrolysis method. (b) Cyclic voltammetries of BNTA, Ti/Ir, and BDD electrodes in 30 mM Na_2SO_4. (c) Enlarge figure of specific area in figure (b). The x-intercepts of the dash lines show the onset potentials for oxygen evolution, which are 2.81 for BNTA and 2.88 V_{RHE} for BDD electrode.

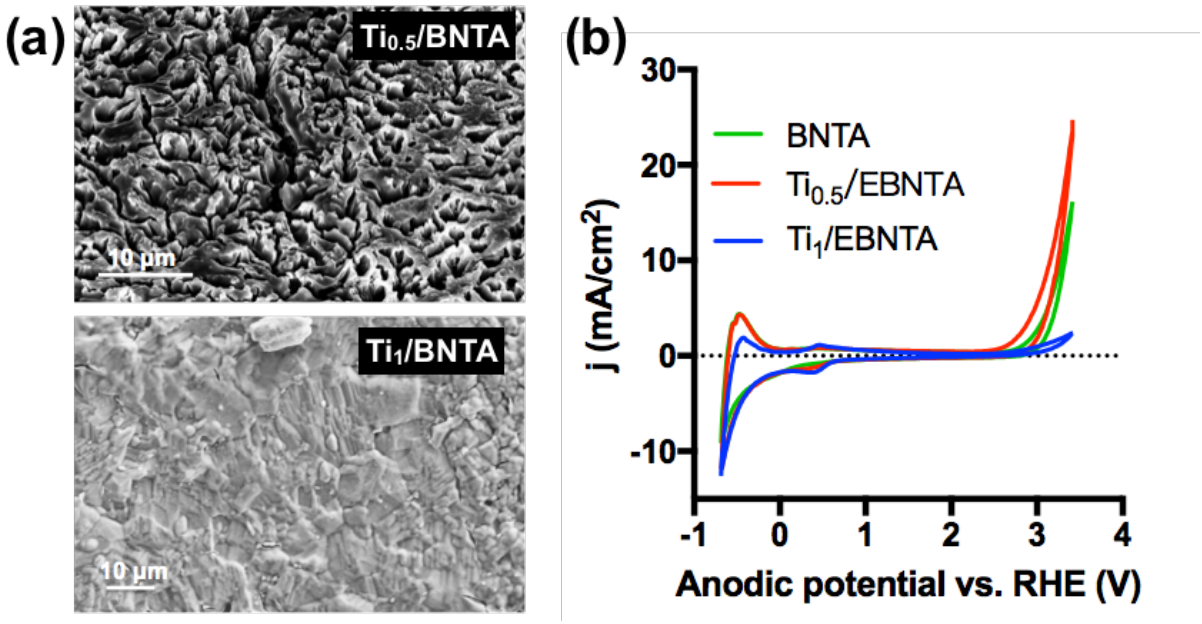

Figure S2. (a) FESEM images of $Ti_{0.5}$/BNTA and Ti_1/BNTA. (b) Cyclic voltammetries of BNTA, $Ti_{0.5}$/BNTA, and Ti_1/BNTA in 30 mM Na_2SO_4.

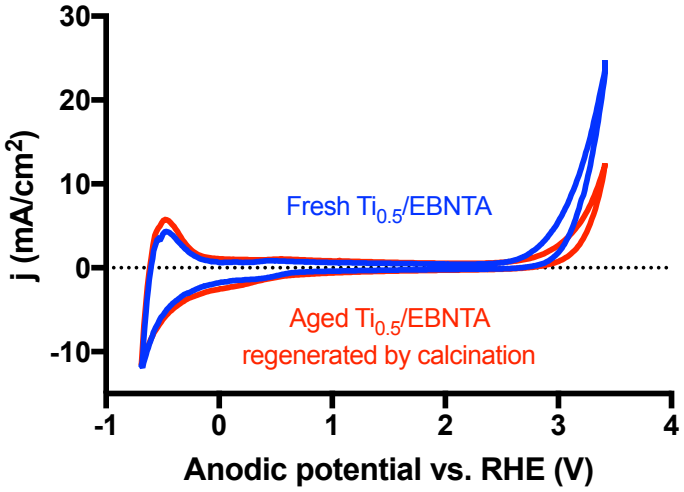

Figure S3. Cyclic voltamagrams of fresh $Ti_{0.5}$/BNTA and aged $Ti_{0.5}$/BNTA regenerated by calcination (450 °C for 1 h) in 30 mM Na_2SO_4. Deactivated $Ti_{0.5}$/EBNTA showed no current response at anodic branch (data not shown).

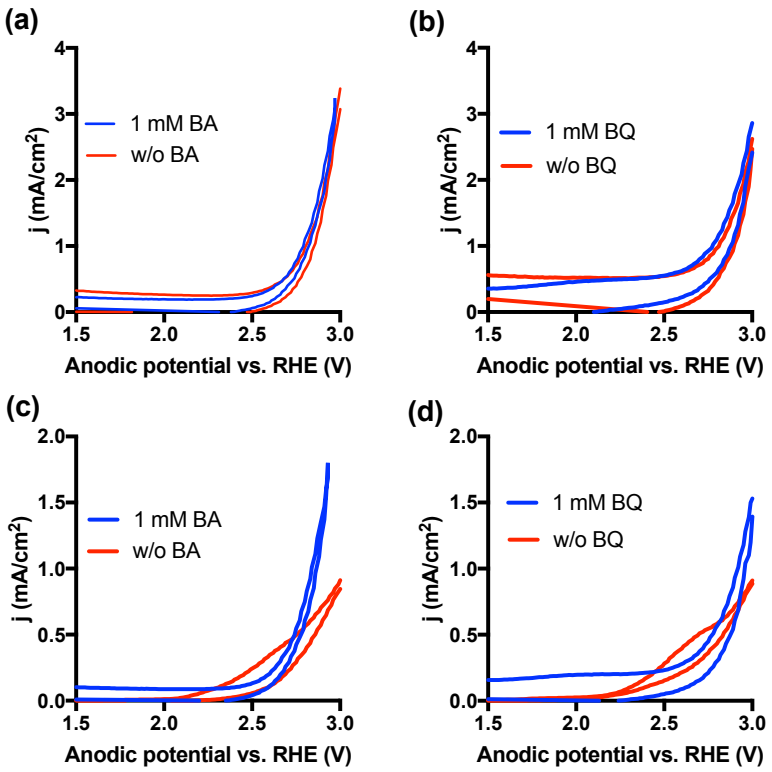

Figure S4. Cyclic voltammetries of (a, b) BNTA and (c,d) BDD electrodes in $NaClO_4$ electrolyte in the presence and absence of probe molecules. Direct electron transfer oxidation contributes to the degradation of BA and BQ on BDD electrode, as sharp increase of current response was observed in the presence of these organics. Such phenomenon were not observed on EBNTA electrode, which rule out the possibility of direct electron transfer oxidation.

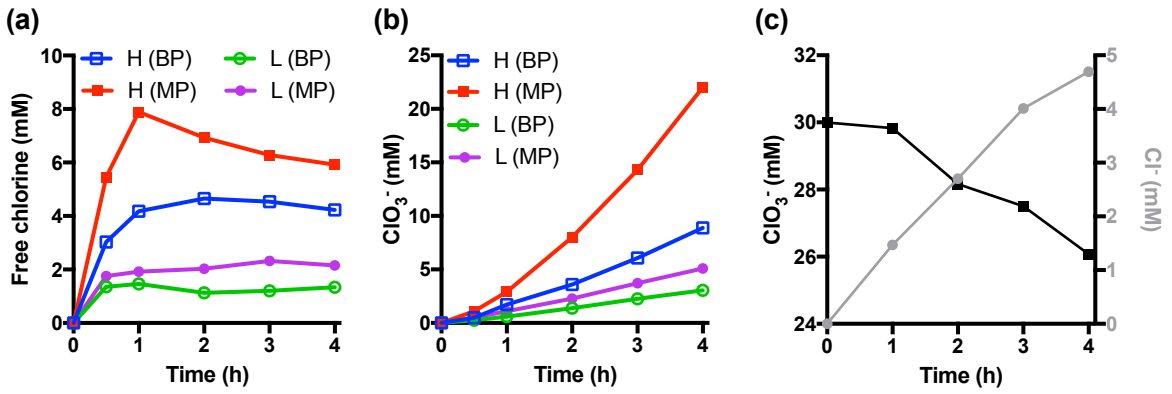

Figure S5. The evolution of (a) free chlorine and (b) ClO_3^- in 30 mM NaCl as a function of electrolysis time at various current density (H: 10 and L: 5 mA/cm^2). (c) Reduction of ClO_3^- to Cl^- in 30 mM $NaClO_3$ at 10 mA/cm^2. In this reaction Pt foil was used as anode and $Ti_{0.5}$/EBNTA was served as cathode. It is found that ClO_3^- gradually decreases accompanied with the increase of Cl^- concentration. This result indicate the reduction of ClO_3^- to Cl^- on $Ti_{0.5}$/EBNTA cathode.

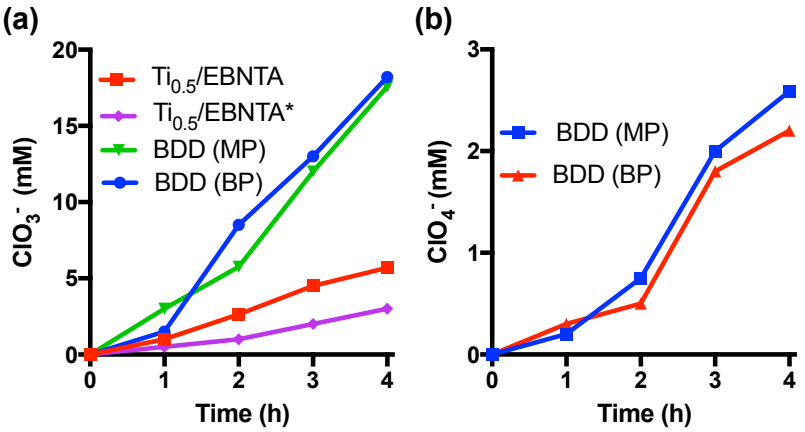

Figure S6. Formation of ClO_3^- and ClO_4^- in the course of human wastewater electrolysis.

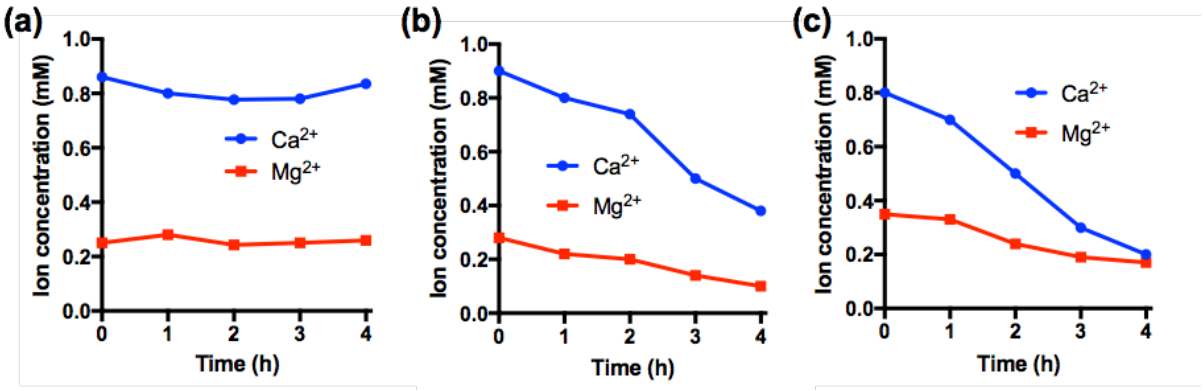

Figure S7. Removal Ca^{2+} and Mg^{2+} during wastewater electrolysis with (a) $Ti_{0.5}$/EBNTA in BP mode, (b) Ti/Ir in MP mode, and (c) BDD in MP mode at 5 mA/cm^2.

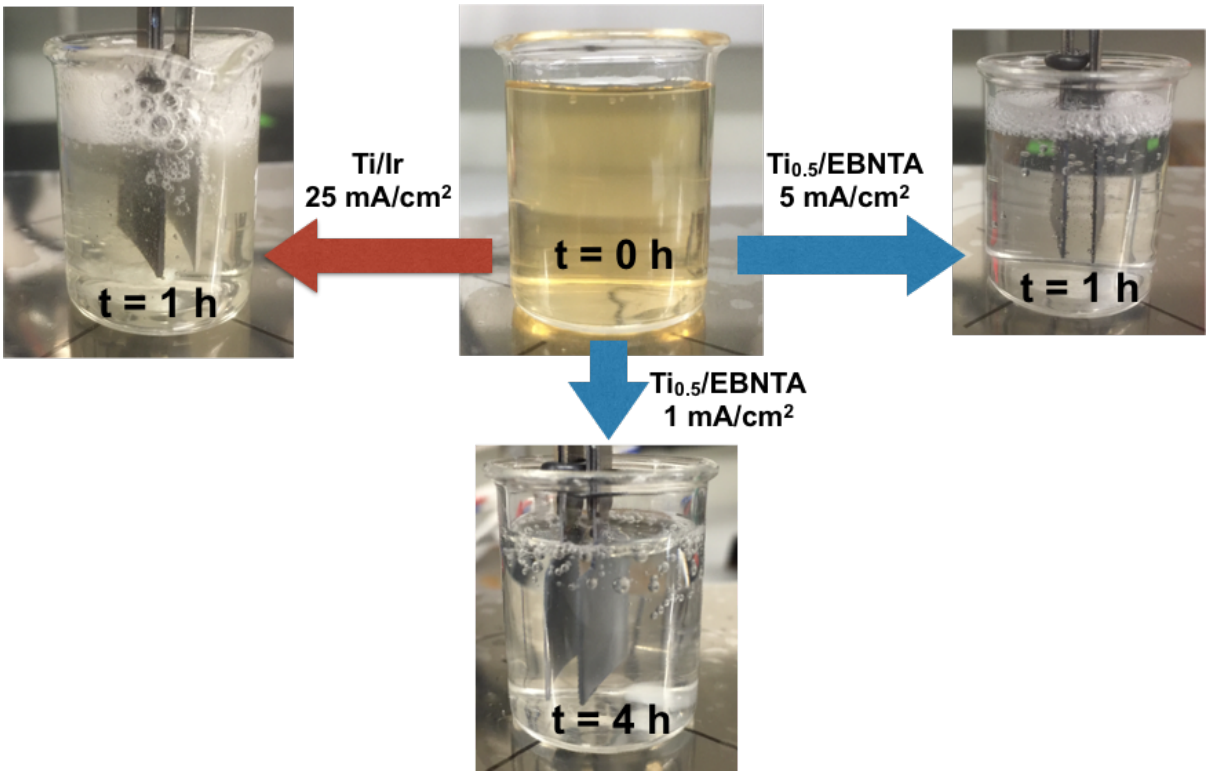

Figure S8. Photo illustrations of foaming during human wastewater electrolysis.

Table S1. Energy consumption of the reported electrochemical treatment of actual wastewater.

Coating	Wastewater	Conductivity (mS/cm)	Energy consumption (kWh/kg COD)	Ref
Bi-TiO_2/Ir	Human wastewater	4-21	96-320	1
Bi-TiO_2/Ir	Human wastewater	1-24	200	2
PbO_2	Dye wastewater	-	242-1030	3
BDD	Reverse osmosis concentrate	6.01	290-340	4
BDD	Urban wastewater	0.77	829-1405	5
BDD	Coking wastewater	2	64	6
BDD	Landfill leachates	9.4	53-94	7
$Ti_{0.5}$/EBNTA	Human wastewater	3.2	67	This study

Text S1. Band structure determination

The Fermi level (E_F) of n-type semiconductor can be approximately treated as the conduction band edge,[8] and flat band potential (E_{FB}) is equal to E_F.[9] It is known that the E_F of NTA is 0.35 V_{SHE}, which can be considered as the conduction band edge (E_C). By adding the 3.2 eV band-gap to E_C, the valence band edge E_V of NTA is determined as 3.65 V_{SHE}. Knowing that there is a 0.1 eV shift of E_V, the E_V of BNTA is determined as 3.55 V_{SHE}. The E_C of BNTA is obtained by adding 3.3 eV band gap to E_V, which is 0.25 V_{SHE}.

Text S2. Calculation of the width of the space charge layer

Flat band potential can be obtained from Mott-Schottky equation

$$\frac{1}{C_{SC}^2} = (\frac{2}{e\varepsilon_0\varepsilon N_D A^2})(E - E_{FB} - \frac{k_B T}{e}) \quad \text{(S1)}$$

Where C_{SC} is the space charge layer capacity (F); e is the elementary electron charge (1.6×10^{-19} C); ε_0 is the permittivity of vaccuum (8.86×10^{-10} F cm^{-1}); ε is the dielectric constant of anatase TiO_2 (31);[10] N_D is the donor state density (cm^{-3}); A is the electrode area; E is the applied bias potential; E_{FB} is the flat band potential; k_B is the Boltzmann constant (1.38×10^{-23} J K^{-1}); T is the temperature (298 K). A plot of $1/C_{SC}^2$ against E should yield a straight line, from which the E_{FB} can be determined from the intercept on E axis. The N_D can be obtained from the slope.

Considering the space charge layer as parallel plate capacitor

$$C_{SC} = \frac{\varepsilon_0 \varepsilon A}{d_{SC}} \quad \text{(S2)}$$

Substituting equation S2 into S1 gives the equation to estimate the width of space charge layers d_{SC}[11, 12]

$$d_{SC} = \left[\frac{2\varepsilon_0 \varepsilon (E - E_{FB})}{eN_D} \right]^{1/2} \quad \text{(S3)}$$

Text S3. Lifetime estimation

An empirical equation for the prediction of lifetime of water oxidation electrode has been proposed previously[13, 14]

$$T_1 \times i_1^n = T_2 \times i_2^n \quad \text{(S4)}$$

where T_1 is lifetime obtained at high current density (i_1). T_2 and i_2 are actual lifetime and current density in operational mode, respectively. n is a coefficient.

As shown in Figure 2, the lifetime of BNTA is 0.5 and 3 h at 20 and 10 mA/cm^2, respectively. Therefore n in equation S4 is calibrated as 2.6 for BNTA electrode. According to equation S4, the 7 h life time (T_1) at 20 mA/cm^2 (i_1) gives the actual lifetime of 42, 257, and 16895 h at current density of 10, 5, and 1 mA/cm^2.

One must notice that these tests are not the typical accelerated life time tests, in which i_1 could be as high as 1 A/cm^2.[13, 14] Because BNTA is inactive for water oxidation, thus operating it at 1 A/cm^2 will instantly leads to an extremely high anodic potential, which consequently results in the corrosion of Ti metal substrate.

References

1. Cho, K.; Qu, Y.; Kwon, D.; Zhang, H.; Cid, C. m. A.; Aryanfar, A.; Hoffmann, M. R. Effects of Anodic Potential and Chloride Ion on Overall Reactivity in Electrochemical Reactors Designed for Solar-Powered Wastewater Treatment. *Environ. Sci. Technol.* **2014**, *48* (4), 2377-2384.
2. Cho, K.; Kwon, D.; Hoffmann, M. R. Electrochemical Treatment of Human Waste Coupled with Molecular Hydrogen Production. *RSC Adv.* **2014**, *4* (9), 4596-4608.
3. Panizza, M.; Cerisola, G. Electrochemical Degradation of Methyl Red Using BDD and PbO2 Anodes. *Ind. Eng. Chem. Res.* **2008**, *47* (18), 6816-6820.
4. Bagastyo, A. Y.; Batstone, D. J.; Kristiana, I.; Gernjak, W.; Joll, C.; Radjenovic, J. Electrochemical Oxidation of Reverse Osmosis Concentrate on Boron-Doped Diamond Anodes at Circumneutral and Acidic pH. *Wat. Res.* **2012**, *46* (18), 6104-6112.
5. Dominguez-Ramos, A.; Irabien, A. Analysis and Modeling of the Continuous Electro-oxidation Process for Organic Matter Removal in Urban Wastewater Treatment. *Ind. Eng. Chem. Res.* **2013**, *52* (22), 7534-7540.
6. Zhu, X.; Ni, J.; Lai, P. Advanced Treatment of Biologically Pretreated Coking Wastewater by Electrochemical Oxidation Using Boron-doped Diamond Electrodes. *Wat. Res.* **2009**, *43* (17), 4347-4355.
7. Anglada, A.; Ortiz, D.; Urtiaga, A.; Ortiz, I. Electrochemical Oxidation of Landfill Leachates at Pilot Scale: Evaluation of Energy Needs. *Wat. Sci. Technol.* **2010**, *61* (9), 2211-2217.
8. Lim, J.; Murugan, P.; Lakshminarasimhan, N.; Kim, J. Y.; Lee, J. S.; Lee, S.-H.; Choi, W. Synergic Photocatalytic Effects of Nitrogen and Niobium Co-Doping in TiO2 for the Redox Conversion of Aquatic Pollutants Under Visible Light. *J. Catal.* **2014**, *310*, 91-99.

9. Grätzel, M. Photoelectrochemical Cells. *Nature* **2001**, *414* (6861), 338-344.

10. Tang, H.; Prasad, K.; Sanjines, R.; Schmid, P.; Levy, F. Electrical and Optical Properties of TiO_2 Anatase Thin Films. *J. Appl. Phys.* **1994**, *75* (4), 2042-2047.

11. Beranek, R.; Tsuchiya, H.; Sugishima, T.; Macak, J.; Taveira, L.; Fujimoto, S.; Kisch, H.; Schmuki, P. Enhancement and Limits of the Photoelectrochemical Response from Anodic TiO_2 Nanotubes. *Appl. Phys. Lett.* **2005**, *87* (24), 243114.

12. van de Krol, R.; Goossens, A.; Schoonman, J. Spatial Extent of Lithium Intercalation in Anatase TiO_2. *J. Phys. Chem. B* **1999**, *103* (34), 7151-7159.

13. Hine, F.; Yasuda, M.; Noda, T.; Yoshida, T.; Okuda, J. Electrochemical Behavior of the Oxide - Coated Metal Anodes. *J. Electrochem. Soc.* **1979**, *126* (9), 1439-1445.

14. Chen, X.; Chen, G.; Yue, P. L. Stable Ti/IrO_x-Sb_2O_5-SnO_2 Anode for O_2 Evolution with Low Ir Content. *J. Phys. Chem. B* **2001**, *105* (20), 4623-4628.